CONEM 2016
CONGRESSO NACIONAL DE ENGENHARIA MECÂNICA
21 - 25 AGOSTO DE 2016
FORTALEZA - CEARÁ

DYNAMIC MODELS OF PARALLEL MECHANISMS USING POWER FLOW APPROACH

Allan Nogueira de Albuquerque, allan@puc-rio.br[1]
Mauro Speranza Neto, msn@puc-rio.br[1]
Marco Antonio Meggiolaro, meggi@puc-rio.br[1]

[1]Pontifical Catholic University – Department of Mechanical Engineering, Mechatronic System Development Laboratory. Rua Marquês de São Vicente, 225, Gávea, CEP 22451-900, Rio de Janeiro, RJ.

Abstract*. This paper presents a procedure for the determination of the analytical form of dynamic models of parallel - or closed kinematic chains - mechanisms through the characterization of the power flow between its components. From the geometrical relations associated to the displacement of their degrees of freedom, the kinematic relations associated to their velocities are determined. Considering the power flow between the degrees of freedom, and also, if necessary, between these and the actuating elements (e.g. electric motors or hydraulic actuators) the equilibrium relations of the forces and torques are obtained. Finally, accounting for inertial effects of system components and, if necessary, the stiffness and damping effects, the equations of motion or the state equations are analytically determined and represented in any reference frame, local or global. This approach adopts the same fundamentals, concepts and elements of the Bond Graph Technique. As an illustration, the procedure is applied in a parallel planar mechanism with three degrees of freedom. The analytical equations lead to a more efficient simulation process and real-time control of these systems.*

Keywords*: Parallel Mechanisms Dynamics, Kinematic Relations, Power Flow, Equilibrium Relations, Bond Graphs.*

1. INTRODUCTION

Mechanisms are mechanical devices composed of links connected by joints, forming open or closed mobile chains. Mechanisms are used in almost every machine to transfer motion or force. Conveyors, part handling systems, printers and vehicle suspension systems are some of the mechanisms applications (Chironis, 1991).

1.1. Parallel mechanisms

Mechanisms are essentially (but not exclusively) made up of multiple rigid bodies that have relative motion between themselves. Each rigid body is connected through a joint to one or more bodies, wherein the serial sequence of connected bodies is called kinematic chain. Open kinematic chains have no restrictions on their ends, as closed chains have restrictions on both ends. Figure 1 shows the differences between the types of kinematic chain. In this work, the focus will be given on the study of mechanisms with closed kinematic chains.

Parallel systems have great advantages when compared to serial manipulators, as better stability and accuracy, ability to handle relatively large loads, high velocities and accelerations and low power operation. The design of parallel manipulators dates back several decades ago, in 1962, when Gough and Witehall designed a parallel system to be used in a universal test machine. Stewart, in 1965, designed a platform to be used in flight simulators. Since then, there have been numerous studies by many researchers. Figure 2.a shows the first flight simulator with a structure of six degrees of freedom and Figure 2.b shows a parallel manipulator used in parts assembling, also with six degrees of freedom (Tapia *et al*., 2009). Parallel manipulators can also be classified as planar, spherical or spatial according to the geometric and motion characteristics (Fig. 3).

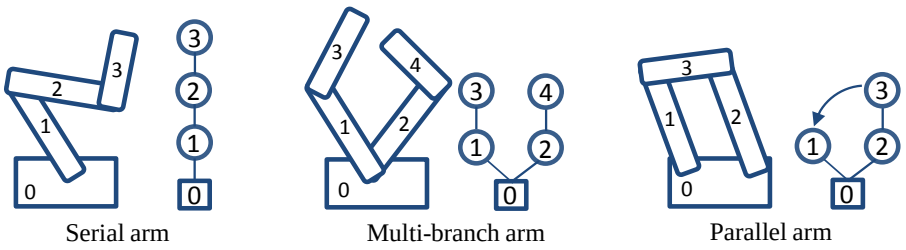

a) **b)** **c)**

Figure 1. Types of kinematic chains: a) serial (open); b) multi-branch; c) parallel (closed).

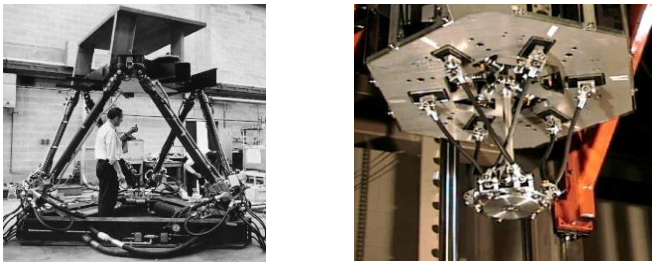

a) **b)**

Figure 2. Stewart platform based mechanisms examples: a) flight simulator; b) assembly robot.

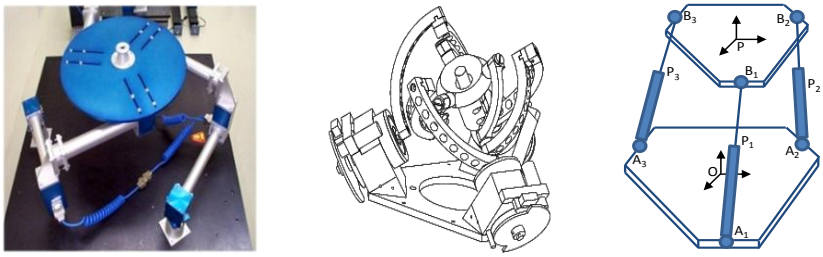

a) **b)** **c)**

Figure 3. Parallel manipulators classification according to its movements: a) planar; b) spherical; c) spatial.

The improvement in the modeling of parallel mechanisms also contributes to solve problems associated with some serial robots tasks. In some tasks, such as when a serial robotic arm opens a door or engages its end effector to a surface or object, the kinematic chain, due to the appearance of restrictions in the degrees of freedom of the end effector, is temporarily closed (Bennett *et al.*, 1991). Another case in which a serial mechanism becomes a closed kinematic chain is the case of the legs of an anthropomorphic robot. When both feet found a restriction (such as the floor, for example), the kinematic chain closes and thus, to estimate the robot's hip movement in order to balance it, multi-branch mechanisms or parallel mechanisms modeling techniques are used (Khandelwal *et al.*, 2013).

Some parallel mechanisms, such as the Bricard's octahedron, are similar, in certain configurations, to the molecular structures of certain compounds, such as the carbon skeleton of the cyclohexane molecule (Chai *et al.*, 2009). Thus, the development of a procedure for modeling parallel mechanisms may assist in the study of the behavior of these molecules and even the development of new materials and substances.

Mohamed *et al.* (2005) deals with the kinematics of parallel mechanisms with several closed chains separating the Jacobian matrices of mechanism's active and passive joints. Kim *et al.* (2001) proposed a two-step solution process: cutting operation and paste operation, that is, a restriction is removed and the model works as the kinematic chain was opened, and then a solution that meets the original closed chain is found. In Fischer *et al.* (2001) the Denavit-Hartenberg and Sheth-Uicker notations were used for kinematic modeling of various types of parallel mechanisms, such as the Whitworth quick return mechanism. In Goulin *et al.* (2011) the static modeling of a 3-RPR parallel robot is made by using the graphs theory in the problem topological modeling and in the derivation of the equations of balance, where the mechanical quantities (movements and actions) are described by helicoids (Davies method).

1.2. Power flow approach

Created by H. M. Paynter in the late 50's and developed by D. C. Karnopp and R. C. Rosenberg (Karnopp *et al.*, 1968; Rosenberg *et al.*, 1983 and Karnopp *et al.*, 1990) in the mid-60's, the bond graphs technique are characterized by the physical model representation of a system through a logical graphic, where the energy flow and the system components information are contained (Speranza Neto *et al.*, 2005).

In Costa Neto (2008) the mathematical models of subsystems using power flow were created so that it was possible to implement them as separate and interchangeable modules in a block diagram, coupling them directly, in computational form. The independent modules are tested individually, being possible to separate kinematics and dynamics. The method used to open the algebraic loops of the closed chain mechanisms eliminates the algebraic equations that characterize the loop. Once the module is created, no adjustment needs to be made in the overall structure of the system.

Zhao *et al*. (2012) used the same technique to model the kinematics and dynamics of a Stewart platform. After the kinematic modeling, the dynamic equations of the upper platform were developed using the Newton-Euler method and then, its model in bond graph has been established. An equivalent approach is used to handle the inertial effects of each actuator. In each actuator-valve set of the simulator an independent position closed loop control is coupled. The bond graph model is made using the software *20-sim* and then, several simulations are realized to verify the model. A comparison with experimental tests proved the feasibility and efficiency of the model, whose the method can be used to model other types of parallel mechanisms.

In his work, Yildiz *et al*. (2008) represented the Stewart platform dynamics using a novel spatial visualization form of the bond graphs. This dynamic model includes all the dynamic and gravitational effects such as the linear motor dynamics (used as an actuator) and the viscous friction of the joints. Furthermore, in this work the actuation system and the structure modeling are unified. As this system has many nonlinearities, originated by your non-linear geometry and the gyroscopic forces, the problem of the resulting derivative (forced) causality due to the rigidly coupled inertial elements is approached and the space-state equations are presented.

The proposed methodology is generalized and applicable in any type of mechanism (open or closed, planar or spatial). For a better comprehension of the methodology, a planar case will be discussed in this work. The inverse kinematic model of the closed chain mechanism, which has easy solution when compared to the direct model, can be developed by any known methodology, without the need for a systematic approach. It begins by determining the inverse geometric model and its derivation to obtain the kinematic relations, and therefore the inverse Jacobian matrix. With the inverse kinematic model, the inverse kinematics bond graph is built and, from the cause and effect relations, the direct dynamic model of the mechanism is found. Thus, this methodology (bond graphs or power flow) is more efficient and secure to achieve the dynamic analytical (closed) models of parallel mechanisms.

2. INVERSE KINEMATICS OF THE PLANAR PLATFORM

2.1. Inverse geometry using vector loop

Figure 4 shows a 3-RPR parallel manipulator. Three limbs connects to the mobile platform and the fixed base by rotational joints in points B_i and A_i, i = 1, 2 e 3. To describe its geometry, a referential frame A(X, Y) fixed to the platform base is added and other frame, B(x, y), is coupled to the mobile platform. Another reference frame, C(x_i, y_i), is fixed to each rotational joint, thus having its origin at the point A_i (i = 1, 2 e 3). The z_i axis of this system points from A_i to B_i (direction of the actuator i). For convenience, the origin of the frame B is located at the center of the mobile platform. The position of the mobile platform can be described by the vector $\boldsymbol{p} = [p_X, p_Y]^T = [X, Y]^T$ and by the rotation matrix ${}^{A}R_{B}$.

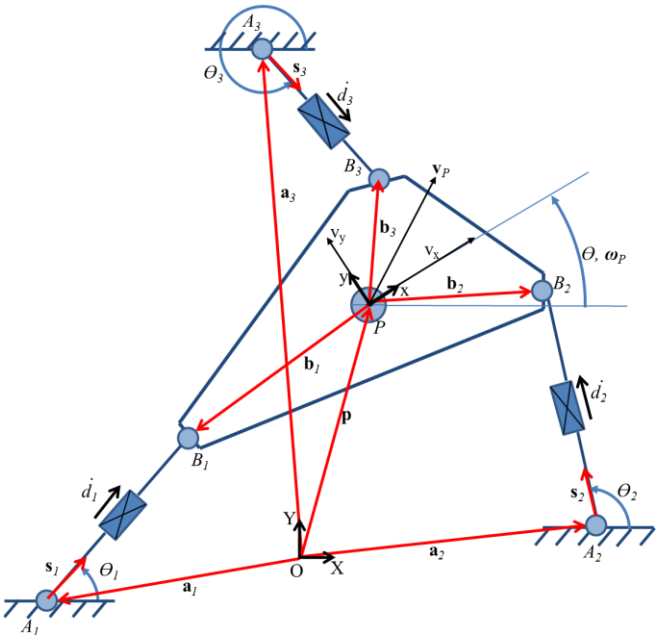

Figure 4. Planar platform with three degrees of freedom.

2.2. Inverse kinematics using vector loop

The velocities state of the mobile platform is defined as a three dimensional vector with the absolute linear velocity and the angular velocity of the mobile platform (Eq. 1).

$$\dot{\boldsymbol{x}} = \begin{bmatrix} \boldsymbol{v}_p \\ \boldsymbol{\omega}_p \end{bmatrix} = \begin{bmatrix} \dot{X} \\ \dot{Y} \\ \dot{\theta} \end{bmatrix} \tag{1}$$

For this manipulator, the input vector is given by $\dot{\mathbf{q}} = [\dot{d_1}, \dot{d_2}, \dot{d_3}]^T$ and the output vector can be described by the centroid velocity *P* and the angular velocity of the mobile platform (Eq. 1). From the vector loop presented in the Fig. 4, the Eq. 2 is obtained.

$$\overline{OP} + \overline{PB_i} = \overline{OA_i} + \overline{A_iB_i} \;\; \therefore \boldsymbol{p} + \boldsymbol{b}_i = \boldsymbol{d}_i + \boldsymbol{a}_i \tag{2}$$

Applying the differential with respect to time, the Eq. 3 is found.

$$\boldsymbol{v}_p + \boldsymbol{\omega}_P \times \boldsymbol{b}_i = d_i(\boldsymbol{\omega}_i \times \boldsymbol{s}_i) + \dot{d}_i \boldsymbol{s}_i \tag{3}$$

in which $\mathbf{b}_i$ and $\mathbf{s}_i$ represent the vector $\overline{PB_i}$ and a unit vector along $\overline{A_iB_i}$, respectively. $\boldsymbol{\omega}_i$ denotes the *i*-th member velocity in relation to the fixed frame *A*. To eliminate $\boldsymbol{\omega}_i$, both sides of Eq. 3 are multiplied for $\mathbf{s}_i$ (Eq. 4).

$$\boldsymbol{s}_i \cdot \boldsymbol{v}_P + \boldsymbol{s}_i(\boldsymbol{\omega}_P \times \boldsymbol{b}_i) = d_i \boldsymbol{s}_i(\boldsymbol{\omega}_i \times \boldsymbol{s}_i) + \dot{d}_i \boldsymbol{s}_i \boldsymbol{s}_i \tag{4}$$

With $\mathbf{s}_i\mathbf{s}_i = 1$, $\mathbf{s}_i(\boldsymbol{\omega}_i \times \mathbf{s}_i) = 0$ and $\mathbf{s}_i(\boldsymbol{\omega}_P \times \mathbf{b}_i) = (\mathbf{b}_i \times \mathbf{s}_i) \cdot \boldsymbol{\omega}_P$, the Eq. 5 is obtained.

$$\boldsymbol{s}_i \cdot \boldsymbol{v}_P + (\boldsymbol{b}_i \times \boldsymbol{s}_i) \cdot \boldsymbol{\omega}_P = \dot{d}_i \tag{5}$$

Thus, one obtains the relationship between the variables which describe the angular and linear velocity of the mobile platform and the velocities of the links of the planar platform (Eq. 5). With this relation, the inverse Jacobian of the manipulator is found (Eq. 6 and Eq. 7).

$$\dot{\boldsymbol{q}} = J^{-1}\dot{\boldsymbol{x}} = \begin{bmatrix} \frac{\partial d_1}{\partial X} & \frac{\partial d_1}{\partial Y} & \frac{\partial d_1}{\partial \theta} \\ \frac{\partial d_2}{\partial X} & \frac{\partial d_2}{\partial Y} & \frac{\partial d_2}{\partial \theta} \\ \frac{\partial d_3}{\partial X} & \frac{\partial d_3}{\partial Y} & \frac{\partial d_3}{\partial \theta} \end{bmatrix} \dot{\boldsymbol{x}} \tag{6}$$

$$J^{-1} = \begin{bmatrix} \boldsymbol{s}_1^T & (\boldsymbol{b}_1 \times \boldsymbol{s}_1)^T \\ \boldsymbol{s}_2^T & (\boldsymbol{b}_2 \times \boldsymbol{s}_2)^T \\ \boldsymbol{s}_3^T & (\boldsymbol{b}_3 \times \boldsymbol{s}_3)^T \end{bmatrix} \tag{7}$$

Equations 8 to 10 shows the dismembering of the terms $\mathbf{s}_i^T$.

$$\boldsymbol{s}_1^T = \frac{\overline{A_1B_1}^T}{d_1} = \begin{bmatrix} \frac{d_1 \cos\theta_1}{d_1} & \frac{d_1 \sin\theta_1}{d_1} \end{bmatrix} = [\cos\theta_1 \quad \sin\theta_1] \tag{8}$$

$$\boldsymbol{s}_2^T = \frac{\overline{A_2B_2}^T}{d_2} = \begin{bmatrix} \frac{d_2 \cos\theta_2}{d_2} & \frac{d_2 \sin\theta_2}{d_2} \end{bmatrix} = [\cos\theta_2 \quad \sin\theta_2] \tag{9}$$

$$\boldsymbol{s}_3^T = \frac{\overline{A_3B_3}^T}{d_3} = \begin{bmatrix} \frac{d_3 \cos\theta_3}{d_3} & \frac{d_3 \sin\theta_3}{d_3} \end{bmatrix} = [\cos\theta_3 \quad \sin\theta_3] \tag{10}$$

The cross product $\boldsymbol{b}_i \times \boldsymbol{s}_i$ is obtained transforming the first vector into a 3 x 3 antisymmetric matrix. Equation 11 presents the result of this cross product and, in Eq. 12, Eq. 6 is rewritten with the inverse Jacobian terms.

$$\boldsymbol{b}_i \times \boldsymbol{s}_i = \widetilde{\boldsymbol{b}}_i \boldsymbol{s}_i = \begin{bmatrix} 0 & 0 & b_{iY} \\ 0 & 0 & -b_{iX} \\ -b_{iY} & b_{iX} & 0 \end{bmatrix} \begin{bmatrix} \cos\theta_i \\ \sin\theta_i \\ 0 \end{bmatrix} = \begin{bmatrix} 0 \\ 0 \\ -b_{iY}\cos\theta_i + b_{iX}\sin\theta_i \end{bmatrix} \tag{11}$$

$$\begin{bmatrix}\dot{d}_1\\ \dot{d}_2\\ \dot{d}_3\end{bmatrix}=\begin{bmatrix}cos\,\theta_1 & sin\,\theta_1 & -b_{1Y}\,cos\,\theta_1+b_{1X}\,sin\,\theta_1\\ cos\,\theta_2 & sin\,\theta_2 & -b_{2Y}\,cos\,\theta_2+b_{2X}\,sin\,\theta_2\\ cos\,\theta_3 & sin\,\theta_3 & -b_{3Y}\,cos\,\theta_3+b_{3X}\,sin\,\theta_3\end{bmatrix}\begin{bmatrix}\dot{X}\\ \dot{Y}\\ \dot{\theta}\end{bmatrix} \tag{12}$$

in which θ_1, θ_2 and θ_3 are given by Eq. 13 to 15.

$$\theta_1=tan^{-1}\left[\frac{b_{1Y}-a_{1Y}}{b_{1X}-a_{1X}}\right]=tan^{-1}\left[\frac{Y+b_{1x}\,sin\,\theta+b_{1y}\,cos\,\theta-a_{1Y}}{X+b_{1x}\,cos\,\theta-b_{1y}\,sin\,\theta-a_{1X}}\right] \tag{13}$$

$$\theta_2=tan^{-1}\left[\frac{b_{2Y}-a_{2Y}}{b_{2X}-a_{2X}}\right]=tan^{-1}\left[\frac{Y+b_{2x}\,sin\,\theta+b_{2y}\,cos\,\theta-a_{2Y}}{X+b_{2x}\,cos\,\theta-b_{2y}\,sin\,\theta-a_{2X}}\right] \tag{14}$$

$$\theta_3=tan^{-1}\left[\frac{b_{3Y}-a_{3Y}}{b_{3X}-a_{3X}}\right]=tan^{-1}\left[\frac{Y+b_{3x}\,\sin\theta+b_{3y}\,\cos\theta-a_{3Y}}{X+b_{3x}\,\cos\theta-b_{3y}\,\sin\theta-a_{3X}}\right] \tag{15}$$

Rewriting Eq. 13 to 15 in function of $tan(\theta_i)$ and differentiating both sides, Eq. 16 are obtained for i = 1, 2, 3.

$$\frac{d(tan(\theta_i))}{dt}=\frac{d}{dt}\left(\frac{Y+b_{ix}\,sin\,\theta+b_{iy}\,cos\,\theta-a_{iY}}{X+b_{ix}\,cos\,\theta-b_{iy}\,sin\,\theta-a_{iX}}\right) \tag{16}$$

Solving the derivative in both sides of Eq. 16 and manipulating the terms in order to put in evidence the absolute linear velocities and angular velocity of the platform, we obtain the inverse Jacobian that relates these velocities to the angular velocity of each of the members. Equation 17 presents that relation and the Eq. 18 presents the terms of the matrix.

$$\dot{\theta}_i=J_{\theta_i}^{-1}\begin{bmatrix}\dot{X}\\ \dot{Y}\\ \dot{\theta}\end{bmatrix} \tag{17}$$

$$J_{\theta_i}^{-1}=f_i(X,\theta,\theta_i)\begin{bmatrix}-Y-b_{ix}\,s\,\theta-b_{iy}\,c\,\theta+a_{iY}\\ X+b_{ix}\,c\,\theta-b_{iy}\,s\,\theta-a_{iX}\\ X\left(b_{ix}\,c\,\theta-b_{iy}\,s\,\theta\right)+Y\left(b_{ix}\,s\,\theta+b_{iy}\,c\,\theta\right)+b_{ix}^2+b_{iy}^2+a_{iX}\left(b_{iy}\,s\,\theta-b_{ix}\,c\,\theta\right)+a_{iY}\left(-b_{iy}\,c\,\theta-b_{ix}\,s\,\theta\right)\end{bmatrix}^T \tag{18}$$

With $c\theta = cos(\theta)$, $s\theta = sin(\theta)$ and f_i given by Eq. 19.

$$f_i(X,\theta,\theta_i)=\frac{cos^2(\theta_i)}{(X+b_{ix}\,c\,\theta-b_{iy}\,s\,\theta-a_{iX})^2} \tag{19}$$

2.3. Inverse kinematics using power flow approach

As in the bond graph speed restrictions may be imposed directly, one can build the bond graph for the kinematics system analysis before mounting the graph for dynamic analysis. In a graph that correctly describes the kinematics (1 and 0 junctions, transformers and gyrators), the dynamics (capacitors, inertias and resistors) can be imposed without the risk of creating models where the main constraints of mechanical systems are violated: geometric or kinematic ties (Speranza Neto *et al*., 2005).

In this model, speed conditions are imposed by ideal velocity sources, that is, a source of velocity for $\dot{X}$, $\dot{Y}$ and $\dot{\theta}$. Besides these velocities, the others 1 junctions (of common velocities) indicates the linear ($\dot{d}_1$, $\dot{d}_2$ e $\dot{d}_3$) and angular velocities ($\dot{\theta}_1$, $\dot{\theta}_2$ e $\dot{\theta}_3$) of the actuators. Thus, the inverse kinematics of the planar platform via bond graphs is represented as shown in Fig. 5, whereby the modulated transformer type two-port elements indicated by J_{ij}^{-1} and $J_{\theta_{ij}}^{-1}$ represents the matrixes J^{-1} (Eq. 12) and J_{θ}^{-1} (Eq. 18) terms of row i and column j, respectively.

3. DYNAMIC MODEL USING POWER FLOW APPROACH

In this Section, will be presented the planar platform dynamics model from the kinematic model using power flow. At first, only one rigid body will be considered in the dynamic model of the manipulator: the mobile platform (with mass m_P and moment of inertia I_{Pzz}). According to the described in Speranza Neto (2007), the Eq. 20 describes the Newton-Euler equations in that rigid body mobile local frame. The differential equations in the local frame are given in Eq. 21.

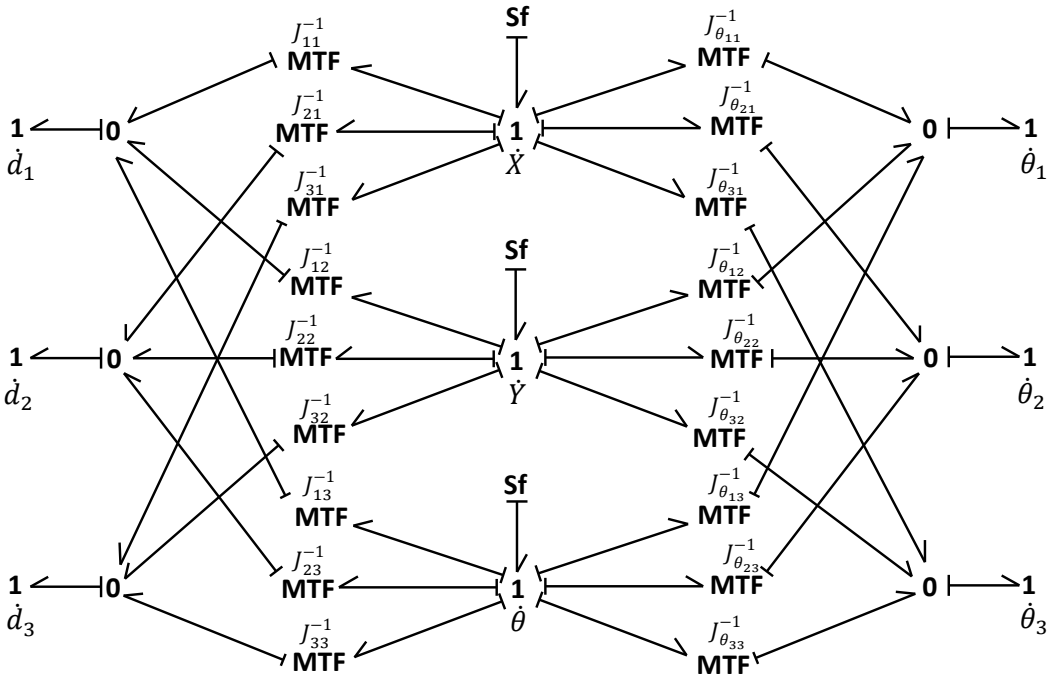

Figure 5. Bond graphs representation of the planar platform inverse kinematics.

$$\begin{cases} \sum F_x = m_P(\dot{v}_x + v_y\omega_z) \\ \sum F_y = m_P(\dot{v}_y - v_x\omega_z) \\ \sum M_z = I_{Pzz}\dot{\omega}_z \end{cases} \tag{20}$$

$$\begin{cases} \dot{v}_x = \frac{\sum F_x}{m_P} - v_y\omega_z \\ \dot{v}_y = \frac{\sum F_y}{m_P} + v_x\omega_z \\ \dot{\omega}_z = \frac{\sum M_z}{I_{Pzz}} \end{cases} \tag{21}$$

According to Speranza Neto (1999), when it can, both completely match the power variables on the inputs and outputs of the subsystems (same type and direction of power flow) and a consistent cause and effect relation (which variables enter and which come out the models to be coupled), the resulting model is fully equivalent to that which would be obtained analytically, allowing your simulation from the simple connection of the modules. Considering this, the diagram (Fig. 6) that illustrates the relationships of cause and effect of the planar platform with three degrees of freedom is mounted.

With the kinematic relationships of this parallel mechanism comes the relation of consequence of the power conservation on the actuators coupling with the rigid body based on the inverse Jacobian (Eq. 6). Equations 22 to 24 present the development of this relation.

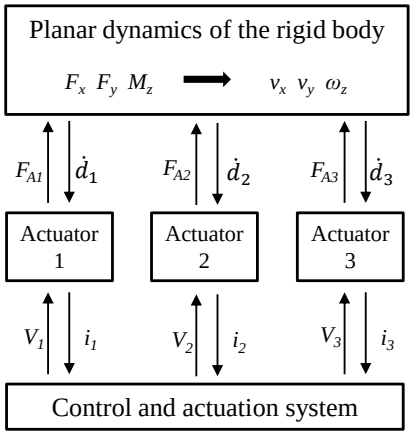

Figure 6. Cause and effect relations of the planar platform.

$$P_{\substack{Rigid\\Body}} = P_{\substack{Actuation\\System}} \Rightarrow [F_x \quad F_y \quad M_z].\begin{bmatrix} v_x \\ v_y \\ \omega_z \end{bmatrix} = [F_1 \quad F_2 \quad F_3].\begin{bmatrix} v_1 \\ v_2 \\ v_3 \end{bmatrix} \tag{22}$$

$$[F_x \quad F_y \quad M_z].\begin{bmatrix} v_x \\ v_y \\ \omega_z \end{bmatrix} = [F_1 \quad F_2 \quad F_3].J^{-1}\begin{bmatrix} v_x \\ v_y \\ \omega_z \end{bmatrix} \tag{23}$$

$$[F_x \quad F_y \quad M_z] = [F_1 \quad F_2 \quad F_3].J^{-1} \Rightarrow \begin{bmatrix} F_x \\ F_y \\ M_z \end{bmatrix} = (J^{-1})^T\begin{bmatrix} F_1 \\ F_2 \\ F_3 \end{bmatrix} \tag{24}$$

Rewriting Eq. 23 in terms of the vectors that contain the velocities (flux) of the actuators ($\overrightarrow{f_A}$) and the platform ($\overrightarrow{f_P}$), Eq. 25 is obtained. Given the relation between the output variables, effort and flow, the relation between the efforts of the actuators and the mobile platform is as shown in Eq. 26.

$$\overrightarrow{f_A} = J^{-1}\overrightarrow{f_P} \tag{25}$$

$$\overrightarrow{e_P} = (J^{-1})^T\overrightarrow{e_A} \tag{26}$$

3.1. Direct dynamics of the planar mechanism using power flow approach

Thereby, the bond graphs structure of the direct dynamics model of the planar platform with three degrees of freedom is shown in Fig. 7. In this, was further added the inertial effects of the bodies that compound the actuators, introducing the terms m_{Ai} and I_{Ai}, which correspond to the mass and moments of inertia of the actuators, with i = 1, 2 and 3. It was also included in this model the viscous friction in the rotation joints of the base (indicated by b_{Ai}, with i = 1, 2 and 3). Besides this, it can also be considered the viscous friction in the B_i joints. In this case, in its constitutive equation will appear the difference in angular velocities θ - θ_i. Figure 8 shows the alteration in the bond graph model for this last case and a scheme showing the involved velocities in detail.

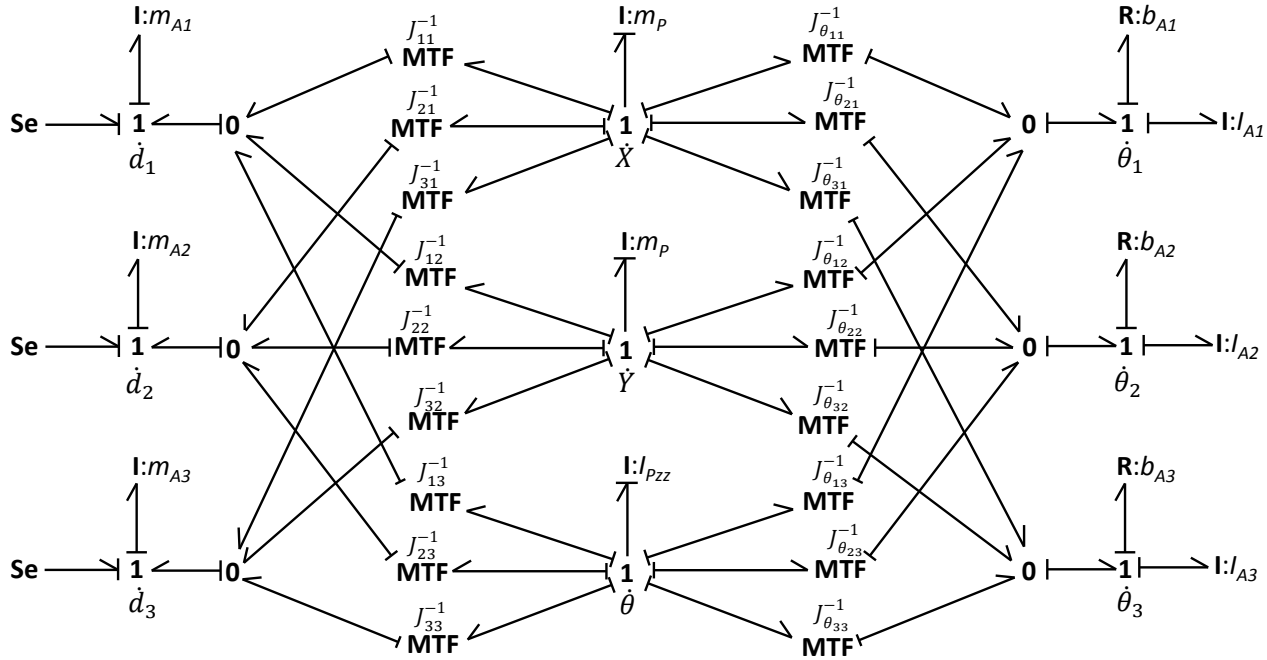

Figure 7. Bond graphs representation of the planar platform dynamics.

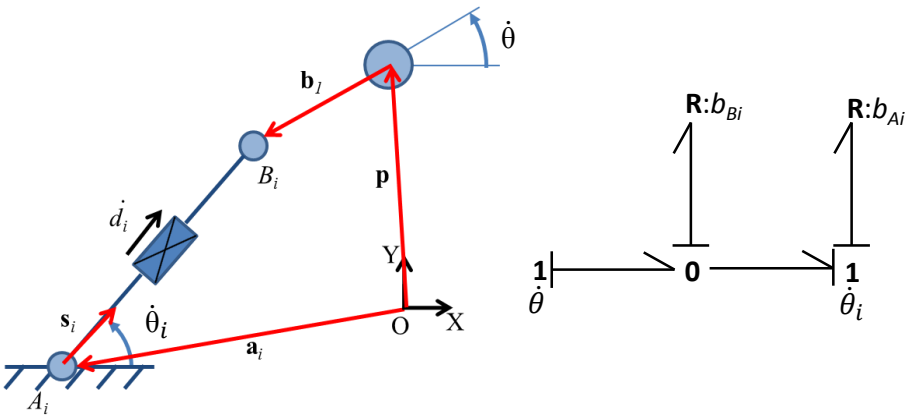

Figure 8. The involved velocities in detail and part of the bond graph model considering the viscous friction in the B_i joints.

3.2. Electric actuator dynamics using power flow approach

The property of modularity, one of the major advantages of the technique, enables the development of complex systems models from simple subsystems (or modules), since these are created predicting the manner in which they will engage each other. This can be done by passive (open) connections or active connections. In the case of the actuation elements (with two or more ports), it is mandatory the use of passive connections, because there is power interaction effectively, resulting in the loading effect, represented in the bond graphs by the causal bar (Speranza Neto *et al*., 2005).

Fig. 9 presents the electric actuator scheme used in this modeling. An electric motor provides power to the actuation system through a torque T_m and an angular velocity ω_m. This power is then transmitted to a leadscrew by a gear set. In bond graphs modeling, motors can, in general, be considered, as effort sources.

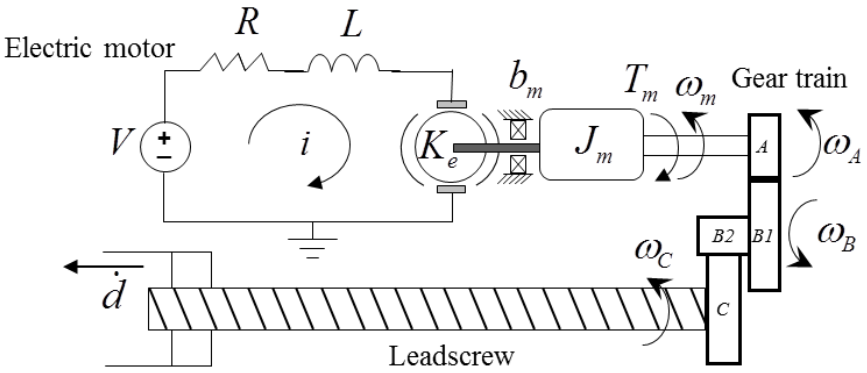

Figure 9. Electric actuator scheme.

From the diagram of Fig. 9, follows that the angular velocity (ω_A) of the gear A, with z_A teeth, is the same velocity of the motor shaft (ω_m). The transmission ratio from gear A to the gear B1, with z_{B1} teeth, is $n_{A\text{-}B1} = z_A/ z_{B1}$. Gears B1 and B2, with z_{B2} teeth, possess the same angular velocity (ω_{B1} and ω_{B2}, respectively). The transmission ratio from gear B2 to C, that have z_C teeth and angular velocity ω_C, is $n_{B2\text{-}C} = z_{B2}/ z_C$. The leadscrew D has the same velocity, ω_C. Through the leadscrew nut, which is coupled to the actuator rod, this movement becomes linear with velocity $\dot{d}$. This relation is given by $n_P = 0{,}5.\pi^{-1}.p.Ne$, where p is the leadscrew pitch and Ne refers to type of thread (single or double). Equation 27 presents the total transmission ratio of the system, where n_e is the transmission ratio between the gears A and C.

$$\dot{d} = n_p.n_{A-B1}.n_{B2-C}.\omega_m = n_p.n_e.\omega_m \tag{27}$$

In this model, were considered the inertia of the motor (J_m), the gear train (J_C), of the actuator rod (m_A) and also the viscous friction coefficients b_m, b_C and b_A associated with these elements. Figure 10 presents the bond graph structure of the actuation system. In the electrical circuit model, R, L and K_e are the resistance, the inductance and the electromagnet constant of the motor, respectively.

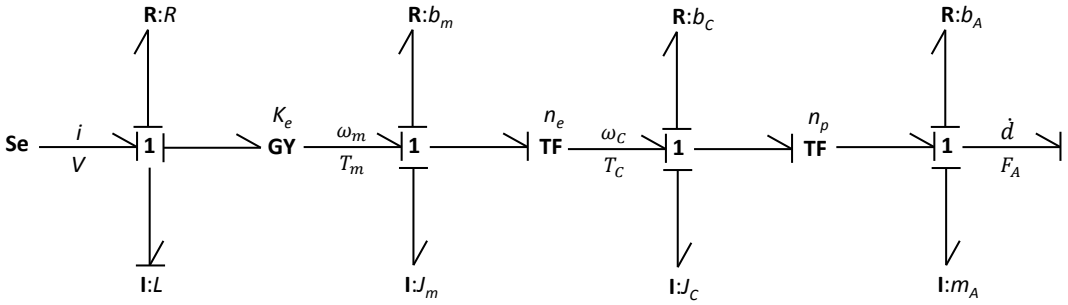

Figure 10. Bond graphs for the electric linear actuator.

3.3. Coupled dynamic model

Figure 11 show the coupled dynamic model represented using the Bond Graph Technique. The actuators model are coupled to the planar platform model through the 1 junctions that represents the actuator output speed, $\dot{d}_i$, with i = 1, 2 and 3.

4. CONCLUSIONS AND FUTURE WORK

In this work a procedure for the determination of the analytical form of dynamic models of a 3-RPR parallel mechanism through the characterization of the power flow between its components was presented. From the geometrical relations associated to the displacement of their degrees of freedom, the kinematic relations associated to their velocities were determined. Considering the power flow between the degrees of freedom and between these and the actuating elements, the equilibrium relations of the forces and torques were obtained. Also, inertial effects of system components, stiffness and damping effects were taken into account and the equations of motion were analytically determined. This approach adopted the same fundamentals, concepts and elements of the Bond Graph Technique.

With this these analytical equations obtained, this leads to a more efficient simulation process and real-time control of these systems. Future works aim at validating the method through the simulation of the complete model and comparison with the experimental data of the manipulator which is under construction.

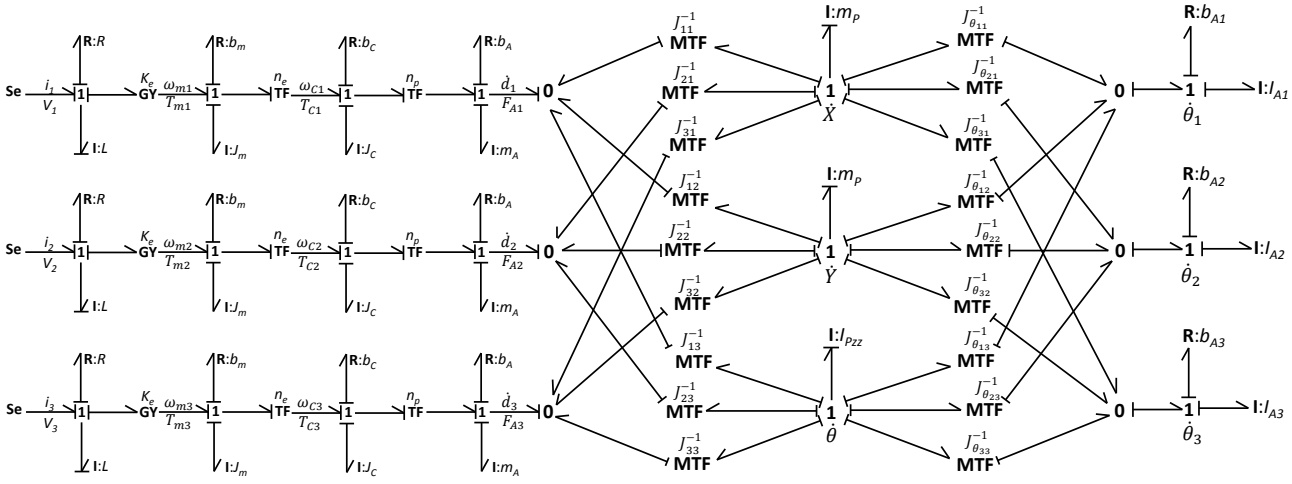

Figure 11. Complete bond graph representation for the 3-PRP parallel mechanism.

5. ACKNOWLEDGEMENTS

The authors of this work would like to thank FAPERJ and CNPq for the financial support.

6. REFERENCES

Bennett, D.J. and Hollerbach, J.M., 1991, "Autonomous calibration of single-loop closed kinematic chains formed by manipulators with passive endpoint constraints", IEEE Transactions on Robotics and Automation, Vol. 7, n° 5.

Chai, W.H. and Chen, Y., 2009, "The line-symmetric octahedral Bricard linkage and its structural closure", School of Mechanics and Aerospace Engineering, Nanyang Technological University, Singapore.

Chironis N., 1991, "Mechanisms and Mechanical Devices". Sourcebook, McGraw-Hill.

Costa Neto, R.T., 2008, "Modelagem e integração dos mecanismos de suspensão e direção de veículos terrestres através do fluxo de potência", *In portuguese*, Pontifical Catholic University, Department of Mechanical Engineering, Doctoral dissertation, Rio de Janeiro, Brazil.

Fischer, I.S. and Chu, T., 2001, "Numerical analysis of the displacement in multi-loop mechanisms", Mechanics Research Communication, vol. 28, n° 2, USA.

Golin, J.F., Martins, D. and Pieri, E.R., 2011, "Modelagem de um manipulador paralelo em contato com um meio rígido através de grafos e helicoides", DINCON 2011, 10th Brazilian Conference on Dynamics, Control and Their Applications, Águas de Lindoia, Brazil.

Karnopp, D.C., Margolis, D.L. and Rosenberg, R.C., 1990, "System dynamics: A unified approach", 2nd Edition, John Wiley & Sons.

Karnopp, D.C. and Rosenberg, R.C., 1968, "Analysis and simulation of multiport systems. The bond graph approach to physical system dynamics", The M.I.T. Press.

Khandelwal, S. and Chevallereau, C., 2013, "Estimate of the trunk attitude of a humanoid by data fusion of inertial sensors and joint encoders", Proceedings of the Sixteenth International Conference on Climbing and Walking Robots, Sydney, Australia.

Kim, J., Kim, K. and Lee, J.Y., 2001, "Solving 3D geometric constraints for closed-loop assemblies", The 5th International Conference on Engineering Design & Automation, Las Vegas, USA.

Mohamed, M.G. and Gosselin, C.M., 2005, "Design and analysis of kinematically redundant parallel manipulators with configurable platforms", IEEE Transactions on Robotics, vol. 21, n° 3, USA.

Rosenberg, R.C. and Karnopp, D.C., 1983, "Introduction to physical system dynamics", McGraw-Hill.

Speranza Neto, M., 1999, "Procedimento para acoplamento de modelos dinâmicos através do fluxo de potência", *In portuguese*, XV Brazilian Congress of Mechanical Engineering, São Paulo, Brazil.

Speranza Neto, M., 2007, "Dinâmica de um corpo rígido através do fluxo de potência", *In portuguese*, Pontifical Catholic University, Department of Mechanical Engineering, Lecture notes, Rio de Janeiro, Brazil.

Speranza Neto, M. and Silva, F.R., 2005, "Modelagem e análise de sistemas dinâmicos", *In portuguese*, Pontifical Catholic University, Department of Mechanical Engineering, Lecture notes, Rio de Janeiro, Brazil.

Tapia, B.C.E. and Méndez, S.J.T., 2009, "Robot paralelo planar para ensamble", División de Estudios de Posgrado e Investigación, Instituto Tecnológico de Puebla, Maravillas, Colombia.

Tsai, L.W., 1999, "Robot analysis – The mechanical of serial and parallel manipulators", Department of Mechanical Engineering and Institute for Systems Research, University of Maryland, John Wiley and Sons, Inc., USA.

Yildiz, I., Ömürlü, V.E. and Sagirli, A., 2008, "Dynamic modeling of a generalized Stewart platform by bond graph method utilizing a novel spatial visualization technique", International Review of Mechanical Engineering, Turkey.

Zhao, Q. and Gao, F., 2012, "Bond graph modelling of hydraulic six-degree-of-freedom motion simulator", Proceedings of the Institution of Mechanical Engineers, Part C: Journal of Mechanical Engineering Science, USA.

7. RESPONSIBILITY NOTICE

The authors are the only responsible for the printed material included in this paper.